determined that the intersystem crossing yields are 0.9 ± 0.1 for 4t-Urd and 1.0 ± 0.1 for DMTU. This is a factor of 45 greater than reported previously for 4t-Urd.

Both oxidative and reductive quenching of the triplet states of 4t-Urd and DMTU have been observed, and the spectra of the anion radicals of 4t-Urd and DMTU and the cation radical of DMTU are reported. These results lead to the conclusion that the first step in the photocrosslinking of 4t-Urd with cytidine in tRNA probably involves an electron transfer. There have been a number of recent reports of the photocrosslinking reactions of nucleic acid bases in DNA with amino acids, such as lysine, in proteins.[50] Our results suggest the possibility of electron-transfer reactions in these systems as well.

Acknowledgment. We thank Dr. Robert Goldbeck for performing the INDO/S calculations and the National Science Foundation for financial support under Grant PMC83-17044.

Registry No. THF, 109-99-9; DMSO, 67-68-5; DMF, 68-12-2; Et_2NPh, 91-66-7; Et_3N, 121-44-8; H_2O, 7732-18-5; MeCN, 75-05-8; EtOH, 64-17-5; 4-thiouridine, 13957-31-8; 1,3-dimethyl-4-thiouracil, 49785-67-3; uracil, 66-22-8; naphthalene, 91-20-3; methylviologen, 1910-42-5; retinol, 68-26-8; (*trans*)-stilbene, 103-30-0.

(50) Saito, I.; Matsuura, T. *Acc. Chem. Res.* **1985**, *18*, 134.

A Microelectrochemical Diode with Submicron Contact Spacing Based on the Connection of Two Microelectrodes Using Dissimilar Redox Polymers

Gregg P. Kittlesen, Henry S. White, and Mark S. Wrighton*

Contribution from the Department of Chemistry, Massachusetts Institute of Technology, Cambridge, Massachusetts 02139. *Received March 18, 1985*

Abstract: Closely spaced, 0.2–1 μm, Au microelectrodes (50 μm long, 1–2 μm wide, and 0.1 μm thick) on Si_3N_4 can be functionalized with poly(vinylferrocene), $PVFc^{+/0}$, or with an *N,N'*-dibenzyl-4,4'-bipyridinium-based polymer, $(BPQ^{2+/+})_n$, derived from hydrolysis of *N,N'*-bis[(*p*-trimethoxysilyl)benzyl]-4,4'-bipyridinium (I). Two- or eight-microelectrode arrays have been functionalized with $PVFc^{+/0}$ or $(BPQ^{2+/+})_n$. Adjacent microelectrodes can be connected with either polymer in the sense that net current can pass from one microelectrode to another, through the polymer, when one electrode is held at a potential where the polymer is oxidized and the other electrode is held at a potential where the polymer is reduced. From such steady-state current an estimate of the diffusion coefficient for charge transport, D_{CT}, in the polymer can be made; values in the range 10^{-9}–10^{-10} cm^2/s are found and accord well with earlier measurements of D_{CT} for the polymers studied. A two-terminal diode can be fabricated by coating one electrode with $(BPQ^{2+/+})_n$ and an adjacent electrode with $PVFc^{+/0}$ such that there is a connection between the microelectrodes via the $(BPQ^{2+/+})_n/PVFc^{+/0}$ contact. Current passes when the applied potential is such that the negative lead is attached to the $(BPQ^{2+/+})_n$-coated electrode and the positive lead is attached to the $PVFc^{+/0}$-coated electrode. When the applied potential approaches the difference in the $E°'$s of the two polymers, current flows with the crucial feature being a downhill (by ~0.9 V) cross redox reaction at the $(BPQ^{2+/+})_n/PVFc^{+/0}$ interface, $BPQ^+ + Fc^+ \rightarrow BPQ^{2+} + Fc^0$. Current does not flow between the microelectrodes when the applied potential is in the opposite sense, because the reaction $BPQ^{2+} + Fc^0 \rightarrow BPQ^+ + Fc^+$ is uphill by ~0.9 V. The switching time of a microelectrochemical diode is controlled by the time required to oxidize and reduce the polymers.

In this article we wish to report procedures that yield the functionalization of two closely spaced (<1 μm) microelectrodes such that each electrode is coated with a different redox polymer in a manner as illustrated in Scheme I. The resulting assembly functions as a diode of the sort first demonstrated by Murray and co-workers.[1] The assembly behaves as a diode in the sense that steady-state current passes in only one direction upon application of a potential across the two electrodes. The principles of such a diode have been demonstrated with macroscopic electrodes derivatized first with one redox polymer followed by a second polymer having a different redox potential and then capped with a porous front contact forming a sandwich structure of metal/polymer/polymer/metal.[1] Our new results demonstrate a synthetic methodology for making an "open-faced" sandwich with a metal-to-metal separation of substantially less than one micron involving a combination of conventional microfabrication techniques and electrochemistry. We recently reported the derivatization of microelectrode arrays using a single polymer, polypyrrole,[2] poly(*N*-methylpyrrole),[3] polyaniline,[4] and poly(3-methyl-

Scheme I. Cross-Sectional View of Redox Polymer Functionalized Microelectrodes[a]

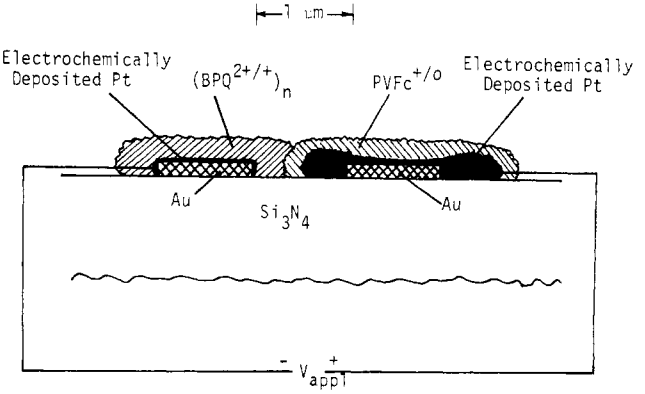

[a] The two-terminal "device" can operate as a diode in the sense that current can pass in only one direction upon application of a potential across the two microelectrodes, since the two polymers have very different redox potentials.

(1) (a) Pickup, P. G.; Murray, R. W. *J. Electrochem. Soc.* **1984**, *131*, 833–839. (b) Pickup, P. G.; Kutner, W.; Leidner, C. R.; Muray, R. W. *J. Am. Chem. Soc.* **1984**, *106*, 1991–1998. (c) Abruna, H. D.; Denisevich, P.; Umana, M.; Meyer, T. J.; Murray, R. W. *J. Am. Chem. Soc.* **1981**, *103*, 1–5. (d) Denisevich, P.; Willman, K. W.; Murray, R. W. *J. Am. Chem. Soc.* **1981**, *103*, 4727–4237.

0002-7863/85/1507-7373$01.50/0

Scheme II. Redox Levels of the $(BPQ^{2+/+/0})_n$ Polymers Relative to a Saturated Calomel Reference Electrode

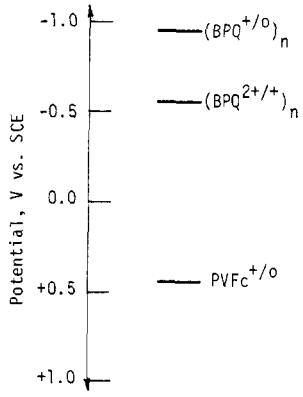

thiophene)[5] and demonstrated that two or more closely spaced microelectrodes could be "connected" in an electrical sense.[2-5] The dramatic change in electrical conductivity of a single connecting polymer with change in its state of charge makes such connected microelectrodes function in a manner analogous to a transistor when the derivatized microelectrode array is immersed in an electrolyte solution.[2-5] In the present work the advance is the demonstration that *two different* redox polymers can be arranged in a way that leads to an aggregate function: a two-terminal diode. The ordered arrangement of molecular materials at the dimensions involved here (surface area of $\sim 10^{-6}$ cm^2) may lead to new ways of duplicating functions found in biological systems, such as photosynthesis, where ordered arrangements of molecular components leads to the useful function characteristic of the assembly.

The fabrication procedures utilized in this work serve to illustrate that it is possible to put *different* polymers on microelectrodes that are very closely spaced (<1 μm). This methodology allows the preparation of microelectrochemical devices that depend on the contact of dissimilar redox polymers and is a general route that can be applied to the preparation of a wide variety of polymer/polymer interfaces. In particular, the polymer/polymer contacts that can be made include situations where the polymer deposited first would be incapable of effecting the electrochemical deposition of the second which is a technique of fabrication used to prepare bilayers on macroscopic electrodes.[1] It is also worth noting that the ability to control the deposition of different polymers on a two-dimensional surface allows a simple procedure for including one, or more, intervening polymers to achieve new kinds of structures and functions, especially chemical sensors.[6]

The keys to achieving diode-like current–voltage characteristics with the device represented in Scheme I are that the (1) only mechanism for passing charge from one metal to the other is via the redox polymers connecting them and (2) redox reaction at the interface between the viologen-based polymer and the ferrocene-based polymer is substantially downhill, resulting in a substantially larger current in one direction than in the other. The viologen-based $(BPQ^{2+/+/0})_n$ is derived from reagent I[7] and the ferrocene-based polymer is poly(vinylferrocene), $PVFc^{+/0}$.[8] In terms of fabricating the assembly in Scheme I and ensuring that the only mechanism for charge transport is via the polymers, it

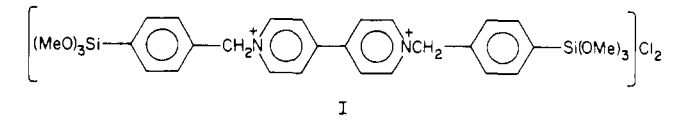

I

is important that each of these polymers[7,8] can be deposited onto electrodes by electrochemical procedures. The redox reaction at the $(BPQ^{2+/+0})_n/PVFc^{+/0}$ interface occurs at a good rate in only one direction because the reactions represented by eq 1 and 2 are thermodynamically downhill by a substantial amount; the reverse reactions are, of course, uphill by the same amount. The $Fc^{+/0}$

$$BPQ^+ + Fc^+ \xrightarrow{k_1} BPQ^{2+} + Fc^0 \quad (1)$$

$$BPQ^0 + Fc^+ \xrightarrow{k_2} BPQ^+ + Fc^0 \quad (2)$$

and $BPQ^{2+/+/0}$ are meant to represent the monomer units of the polymers, in these two equations. At the $(BPQ^{2+/+/0})_n/PVFc^{+/0}$ interface redox reaction between the monomer units is the only mechanism to pass net, steady-state current when there are no other redox active species in the medium in which the device is immersed. Since the processes represented by eq 1 and 2 are so far downhill, Scheme II, only when the $(BPQ^{2+/+0})_n$-coated electrode is the negative electrode will substantial current flow from one microelectrode to the other. The point is that when the $(BPQ^{2+/+/0})_n$-coated electrode is the positive electrode there is no mechanism for charge transfer because Fc^0 is not, realistically, thermodynamically capable of reducing BPQ^{2+}. The equilibrium constants for reactions 1 and 2 exceed 10^{15} and 10^{20}, respectively. The actual extent of the asymmetry in the steady-state current–voltage curves of an electrochemical diode should depend on the difference in $E^{0\prime}$'s of the two polymers, as developed in the work of Murray and co-workers.[1]

The small spacing between the two microelectrodes is crucial to being able to make a device giving conveniently measurable steady-state current. This follows from the very modest redox conductivity of the $(BPQ^{2+/+/0})_n$[9] and $PVFc^{+/0}$.[8] For these materials the maximum conductivity is many orders of magnitude below that of the conducting state of polyaniline, polypyrrole, or poly(3-methylthiophene).[2-5] Consequently, the maximum steady-state current between connected microelectrodes is much less for microelectrodes connected with the $(BPQ^{2+/+/0})_n$ and $PVFc^{+/0}$ redox polymers, and the close spacing of the contacts is necessary to achieve easily detectable current. The charge transport in the $(BPQ^{2+/+/0})_n$[9] and the $PVFc^{+/0}$[8] has been studied with use of macroscopic electrodes and conventional techniques. The funadmental characteristic of importance is a diffusion coefficient for charge transport, D_{CT}; for these redox polymers D_{CT} is $\sim 10^{-9}$–10^{-10} cm^2/s. The low value of D_{CT} signals low conductivity, therefore, low steady-state currents. Also, the small value of D_{CT} indicates that the frequency of turn-on/turn-off of a diode as in Scheme I will be much lower than that for conventional solid-state devices. Accordingly, the small spacing between contacts is important in achieving fast electrochemical switching, in addition to being crucial to achieve significant steady-state currents. Note that the earlier measurements of D_{CT} indicate that detectable currents can be expected from an assembly like that in Scheme I, but the small electrode area involved means that very small currents will be found. Accordingly, we have undertaken the development of methods to close the gap between microelectrodes by electrochemically depositing metals onto microfabricated arrays resulting in submicron electrode separations.

(2) White, H. S.; Kittlesen, G. P.; Wrighton, M. S. *J. Am. Chem. Soc.* **1984**, *106*, 5375–5377.
(3) Kittlesen, G. P.; White, H. S.; Wrighton, M. S. *J. Am. Chem. Soc.* **1984**, *106*, 7389–7396.
(4) Paul, E. W.; Ricco, A. J.; Wrighton, M. S. *J. Phys. Chem.* **1985**, *89*, 1441–1447.
(5) Thackeray, J. W.; White, H. S.; Wrighton, M. S. *J. Phys. Chem.* **1985**, *89*, 5133.
(6) Wrighton, M. S. *Comments Inorg. Chem.* **1985**, *4*, 269–294.
(7) Dominey, R. N.; Lewis, T. J.; Wrighton, M. S. *J. Phys. Chem.* **1983**, *97*, 5346.
(8) (a) Merz, A.; Bard, A. J. *J. Am. Chem. Soc.* **1978**, *100*, 3222–3223. (b) Peerce, P. J.; Bard, A. J. *J. Electroanal. Chem.* **1980**, *108*, 121–125; *112*, 97–115; *114*, 89–115. (c) Daum, Murray, R. W. *J. Phys. Chem.* **1981**, *85*, 389–396. (d) Daum, P.; Lenhard, J. R.; Rolison, D.; Murray, R. W. *J. Am. Chem. Soc.* **1980**, *102*, 4649–4653.
(9) Lewis, T. J.; White, H. S.; Wrighton, M. S. *J. Am. Chem. Soc.* **1984**, *106*, 6947–6952.
(10) (a) Wightman, R. M. *Anal. Chem.* **1981**, *53*, 1125a–1134a. (b) Howell, J. O.; Wightman, R. M. *Anal. Chem.* **1984**, *54*, 534–529. (c) Sutts, K. J.; Dayton, M. A.; Wightman, R. M. *Anal. Chem.* **1982**, *54*, 995–998. (d) Candill, W. L.; Howell, J. O.; Wightman, R. M. *Anal. Chem.* **1982**, *54*, 2532–2535. (e) Dayton, M. A.; Brown, J. S.f Sutts, K. J.; Wightman, R. M. *Anal. Chem.* **1980**, *52*, 946–950. (f) Dayton, M. A.; Ewing, A. G.; Wightman, R. M. *Anal. Chem.* **1980**, *52*, 2392–2395.

Experimental Section

Fabrication of Microelectrode Arrays. Two chip designs were employed: the first possesses two adjacent microelectrodes 1 μm wide separated by 1 μm, and the second possesses eight adjacent microelectrodes ~2 μm wide separated by ~2 μm. Fabrication of the microelectrode arrays was accomplished by previously described methods[2-5] with the following modifications. A 1.01 μm thick thermal oxide was grown on p-Si substrates. A 0.43 μm thick Si_3N_4 film was deposited on the oxidized substrates by low-pressure chemical vapor deposition at 800 °C under flow rates of SiH_2Cl_2 at 27 SCCM and NH_3 at 93 SCCM diluted in N_2 up to a pressure of 330 mtorr.

A 1.4 μm thick layer of KTI-1370 positive photoresist on the nitrided substrate was patterned for metal lift-off. Immediately prior to metal deposition the photoresist-coated substrates were cleaned in an oxygen plasma planar etching chamber at 200W forward power in 60 mtorr of oxygen for 20 s leaving a 1.25 μm thick layer of photoresist. A two-level metallization was performed in a NRC 3117 electron beam evaporation system. A Cr adhesion layer of 60 Å was evaporated followed by 1200 Å of Au. Metal lift-off was achieved in warm acetone.

Epoxy encapsulation of the chip was aided by masking the desired 50 μm length of the microelectrodes with soft-baked positive photoresist. Epoxi-Patch 0151 Clear (Hysol) was applied to each chip to cover the microelectrode leads up to the edge of the photoresist mask with the aid of a Rucker and Kolls XYZ manipulator. The epoxy was partially cured at 70 °C for 1 h. The photoresist mask was then dissolved in warm acetone. The wafer was then cleaned in hot aqueous H_2O_2 (6% by volume)/aqueous NH_3 (14% by volume) for 5 min, rinsed in deionized water, and blown dry with N_2. A final cleaning was performed in an oxygen plasma planar etching chamber at 400W forward power in 60 mtorr of oxygen for 2 min. This encapsulation procedure yielded microelectrodes of reproducible geometry. Die were then separated and packaged. Packaged arrays of microelectrodes were typically cleaned by a negative potential excursion in aqueous electrolyte to evolve H_2 followed by the electrodeposition of Pt from an aqueous solution containing 2 mM K_2PtCl_4 and 0.1 M K_2HPO_4.

Chemicals. OmniSolv CH_3CN (EM Science) was purified and dried by distillation from P_2O_5. Water was triply distilled. The $[n\text{-}Bu_4N]ClO_4$ (Southwestern Analytical) was dried at 70 °C under vacuum for >24 h. $LiClO_4$ (Alfa) and $[Ru(NH_3)_6]Cl_3$ (Strem) were used as received, as was poly(vinylferrocene) (Polysciences, lot No. 45160). Reagent I was previously synthesized and characterized.[7]

Electrochemical Equipment. Electroplating was accomplished with a Princeton Applied Research Model 173 Potentiostat/Galvanostat, Model 179 Digital Coulometer, and Model 175 Universal Programmer. The remaining electrochemical experiments were performed on a Pine Model RDE4 bipotentiostat and recorded on a Kipp & Zonen BD91 x-y-y′ recorder. All potentials were controlled relative to an aqueous saturated calomel reference electrode (SCE). Electrochemical measurements were carried out under N_2 or Ar at 25 °C.

Derivatization of Microelectrodes. Selective deposition of $(BPQ^{2+/+})_n$ on one platinized microelectrode was achieved by cycling the electrode potential between 0.0 and −0.75 V vs. SCE at 50 mV/s in an aqueous solution of 0.5 mM of I and 0.2 M KCl/0.1 M K_2HPO_4 while holding the potential of the adjacent microelectrode at 0.0 V vs. SCE until the desired coverage was obtained. Integration of the charge under the first reduction peak (~−0.55 V vs. SCE) observed in aqueous 1.0 M KCl was used to calculate coverage of $(BPQ^{2+/+})_n$. The $PVFc^{+/0}$ was deposited on the remaining microelectrode by oxidation[8a] at +0.8 V vs. SCE in a solution containing 4 mg of $PVFc^0$ in 5 mL of CH_2Cl_2/5 mM $[n\text{-}Bu_4N]ClO_4$ and removal of the electrode in the oxidized state after passage of the desired amount of charge. Integration of the charge under the oxidation peak (~+0.4 V vs. SCE) observed in CH_3CN/0.1 M $[n\text{-}Bu_4N]ClO_4$ was used to calculate the coverage of electroactive $PVFc^{+/0}$.

Scanning Electron Microscopy. The microelectrode arrays were examined by electron microscopy on a Cambride Mark 2A Stereoscan with a resolution of 20 nm. The arrays were first coated with ~200 Å of Au to minimize problems from surface charging.

Results and Discussion

Electrochemical Characterization and Modification of Microelectrode Arrays by Pt Deposition. The Au microelectrodes used in this study were typically 50 μm long, 1–2 μm wide, and ~0.1 μm thick on an insulating layer of Si_3N_4. General fabrication procedures are given in the Experimental Section and follow closely the methods previously reported.[2-5] The Au microelectrode array consisted of either eight or two microelectrodes spaced ~1 μm from one another. A two-microelectrode chip is illustrated in Figure 1. In our earlier work we had difficulty in obtaining

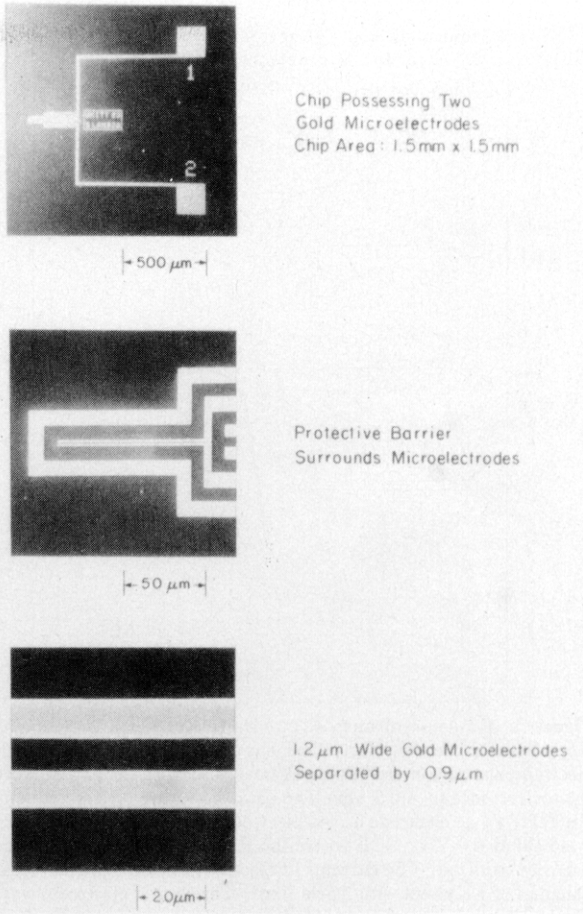

Figure 1. A scanning electron micrograph of the two-electrode array used in this work. The "protective barrier" improves the lift-off procedure used in the microfabrication.

reproducible electrochemical response from each microelectrode. In this work we have been able to obtain reproducible response by electrochemically depositing a small amount of Pt onto each Au electrode. The amount of Pt deposited is ~10^{-6} mol/cm^2. Such "freshened" microelectrodes give reproducible response to solution redox reagents such as aqueous $Ru(NH_3)_6^{3+}$. Since the microelectrodes are small in one dimension (width) the electrochemical response differs from that typically observed at a macroscopic electrode.[10] In particular, in linear potential sweep voltammetry at modest sweep rates and modest redox reagent concentrations the current–voltage curve shows no concentration depletion as is typically found at macroscopic electrodes. Figure 2 illustrates the situation for the reduction of $Ru(NH_3)_6^{3+}$; the current–voltage curve at 50 mV/s shows essentially a steady-state current that we find to be proportional to concentration of $Ru(NH_3)_6^{3+}$. Under the same conditions the response to the $Ru(NH_3)_6^{3+}$ at a macroscopic electrode would be the familiar voltammetric "wave" with a well-defined current peak.[11] The electrochemical deposition of Pt onto the Au microelectrodes gives reproducible surfaces for subsequent modification.

The electrochemical deposition of Pt onto the microelectrodes can be useful in another respect: the deposition of Pt can be used to substantially close the spacing between microelectrodes. A complete account will be given elsewhere, but here we simply note that it is possible to close the spacing between two microelectrodes to ~0.2 μm without yielding an electrical short between adjacent microelectrodes. Figure 3 shows Pt-coated microelectrodes that can be compared to the "naked" Au electrodes illustrated in Figure

(11) Bard, A. J.; Faulkner, L. R. "Electrochemical Methods"; Wiley: New York, 1980.
(12) Pickup, P. G.; Murray, R. W. *J. Am. Chem. Soc.* **1983**, *105*, 4510–4514 and references therein.
(13) Kittlesen, G. P.; Wrighton, M. S. *J. Mol. Electronics*, in press.

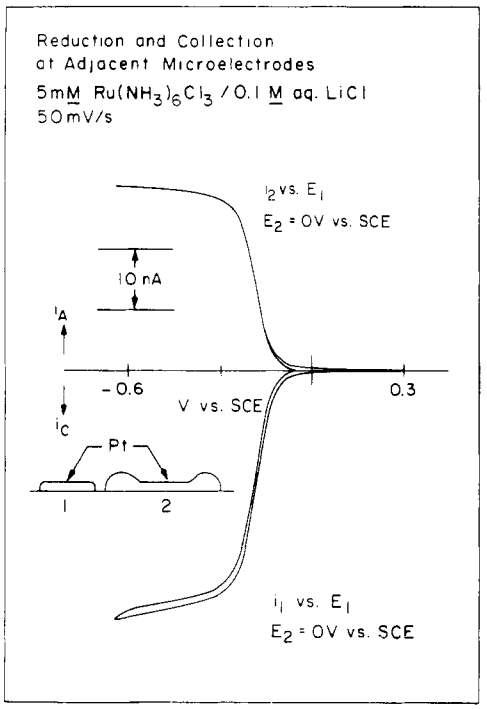

Figure 2. Response of microelectrodes to $Ru(NH_3)_6^{3+/2+}$ in aqueous electrolyte. Note that electrode 1 has been lightly Pt coated and that electrode has been more heavily Pt coated to close the gap between the microelectrodes to ~0.3 μm. The data shown are for the reduction of $Ru(NH_3)_6^{3+}$ at electrode 1. As electrode 1 is swept negative electrode 2 is held at 0.0 V vs. SCE where the $Ru(NH_3)_6^{2+}$ formed at electrode 1 can be oxidized. The currents at electrodes 1 and 2 are shown as the potential of 1 is swept with 2 held fixed. This pair of electrodes was used for the experiments represented by the data summarized in Figures 5–9.

1. Typically, the procedure is to first "freshen" both microelectrodes with a small amount of Pt and then deposit a more substantial amount of Pt onto one of the electrodes. This strategy allows edge definition on the lightly coated microelectrode to be essentially that derived from the conventional microfabrication procedure. The Pt deposited electrochemically, Figure 3, is relatively rough but nonetheless the spacing between microelectrodes can be closed substantially compared to ultraviolet/visible photolithography which underlies the conventional microfabrication procedure used to prepare the arrays. Presumably, the closer the spacing the faster the switching will be between the on and off condition of a diode like that represented in Scheme I.

The microelectrodes of the arrays fabricated are sufficiently closely spaced that the redox products generated at one microelectrode can be detected at another. Thus, a pair of microelectrodes can function in a manner analogous to a rotating ring-disk electrode.[11] As an illustration, consider the information presented in Figure 2. The reduction of $Ru(NH_3)_6^{3+}$ to $Ru(NH_3)_6^{2+}$ occurs at electrode 1 as the potential of electrode 1, E_1, is moved at 50 mV/s from 0.0 to −0.6 V vs. SCE. If the potential of electrode 2, E_2, is fixed at 0.0 V vs. SCE where $Ru(NH_3)_6^{2+}$ can be oxidized

Scheme III. Eight Microelectrodes Connected with a Single Redox Polymer, $PVFc^{+/0}$ [a]

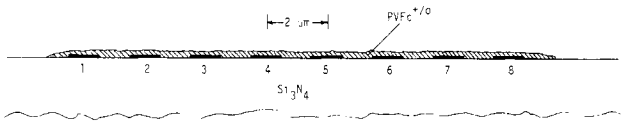

[a] Steady-state current can pass when E_4 is at +0.4 V vs. SCE where the polymer is in the $PVFc^+$ state and E_3 and E_5 are at 0.0 V vs. SCE where the polymer is in the $PVFc^0$ state; cf. Figure 4.

to $Ru(NH_3)_6^{3+}$, anodic current is observed at electrode 2 when E_1 is such that $Ru(NH_3)_6^{2+}$ is produced at electrode 1. The ratio of anodic current at electrode 2 and the cathodic current at electrode 1 is the collection efficiency. For the particular arrangement of microelectrodes used to collect the data in Figure 2 the collection efficiency is ~80%. Note that for the arrangement used the collector electrode, electrode 2, is larger than electrode 1, since Pt has been deposited onto it in an amount consistent with a spacing of about 0.3 μm.

The ability to generate redox products at one microelectrode and detect them at the others has some possible analytical utility which will be elaborated elsewhere. Here we use such generation/collection measurements to characterize the arrays and polymer modified arrays. At this point, it should be emphasized that negligible current passes between two microelectrodes upon application of a potential difference less than the decomposition potential of the medium. Thus, in an aqueous solution of innocent electrolyte the applied potential must be kept below 1.23 V, the decomposition potential of H_2O. When polymer is used to electrically connect microelectrodes, generation/collection experiments can be used to unambiguously establish the mechanism of current flow when there is a potential difference between the two electrodes.

Modification of Microelectrodes with $(BPQ^{2+/+})_n$ or $(PVFc^{+/0})$. The key to being able to fabricate a functioning diode like that represented in Scheme I is to be able to put one polymer, $(BPQ^{2+/+/0})_n$, on one electrode and a second polymer, $PVFc^{+/0}$, on an adjacent electrode in a manner that yields a contact between the two polymers where each electrode is only directly contacted by one of the polymers. Our "synthetic" strategy is to exploit electrochemically assisted deposition procedures[8a,9] to control where polymer is deposited and in what amount.

The $PVFc^{+/0}$ redox polymer can be deposited onto microelectrodes such that adjacent microelectrodes are connected as illustrated in Scheme III. The $PVFc^{+/0}$ redox system can be deposited by oxidative deposition[8a] as outlined in the Experimental Section. Figure 4 gives some data characteristic of microelectrodes connected with $PVFc^{+/0}$. The data are for an eight-electrode array uniformly coated with $PVFc^{+/0}$ at a coverage of ~10^{-8} mol/cm^2. Taking electrode 4 as the "generator" electrode and various combinations of the others as "collector" electrodes it is evident that a sweep of the potential of electrode 4, E_4, from 0.0 to +0.8 V vs. SCE results in a voltammetric wave consistent with the oxidation of $PVFc^0$ to $PVFc^+$. When the collector electrodes are held at 0.0 V vs. SCE, the $PVFc^+$ generated by oxidation at

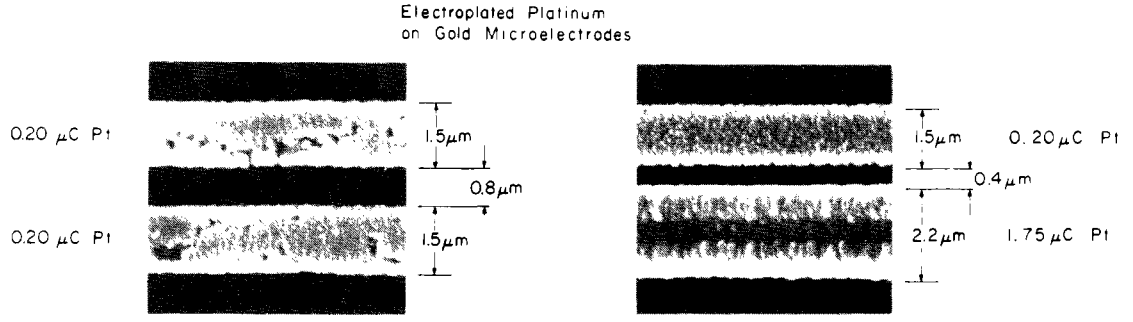

Figure 3. Comparison of Pt-coated adjacent microelectrodes to illustrate the fact that the separation between microelectrodes can be adjusted by Pt deposition.

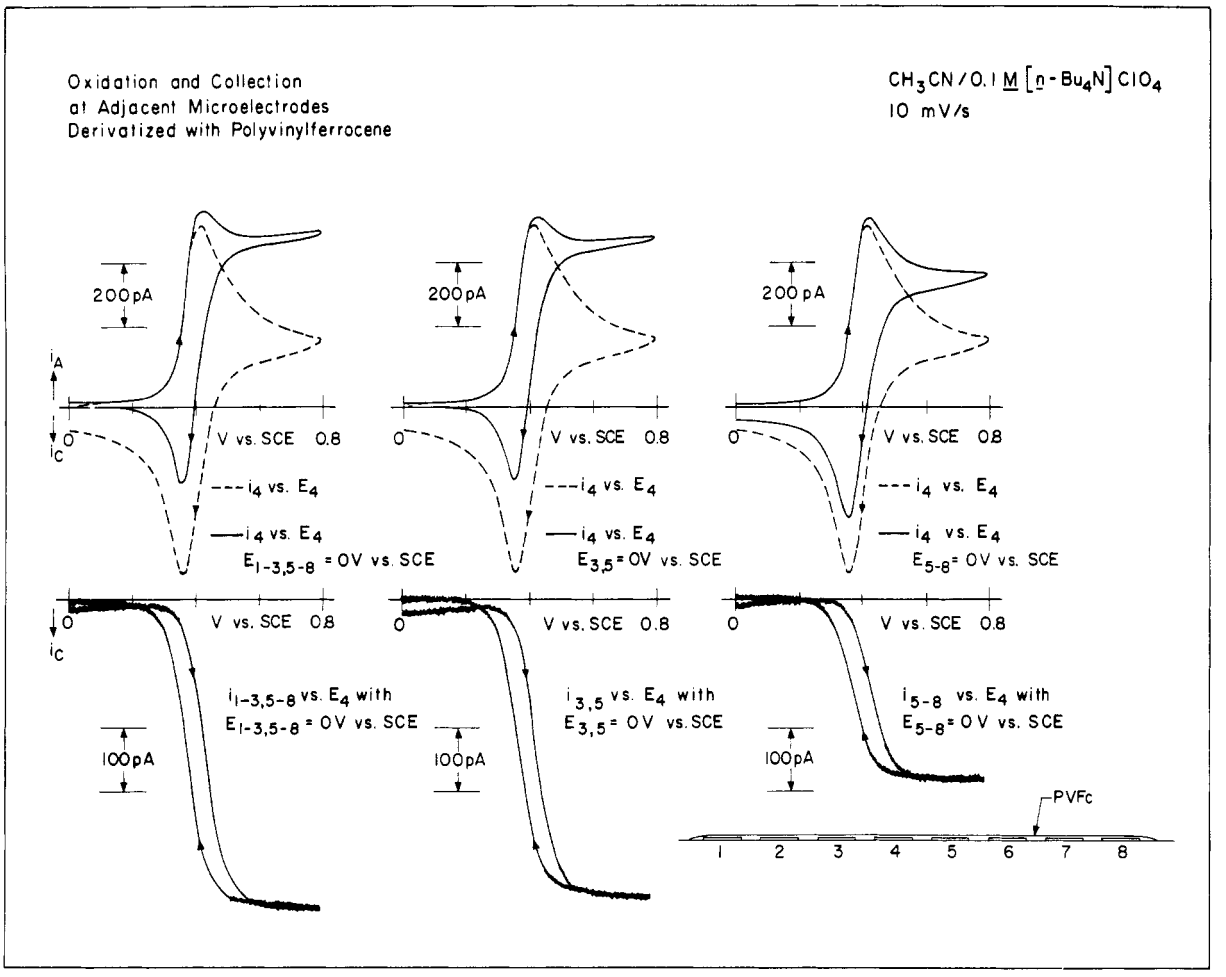

Figure 4. Characterization of an eight microelectrode array coated with a film of $PVFc^{+/0}$. The inset at the lower right shows a cross-sectional view of the microelectrode array. The upper cyclic voltammograms (10 mV/s) are for electrode 4 without potential control of the other microelectrodes (---) and with all other microelectrodes held at 0.0 V vs. SCE (—, left); with electrodes 3 and 5 held at 0.0 V vs. SCE and the others without potential control (—, middle); and with electrodes 5–8 held at 0.0 V vs. SCE and the others without potential control, (—, right). The curves below the cyclic voltammograms show the cathodic current for the indicated "collector" electrodes as the potential of the "generator" electrode 4 is cycled between 0.0 and +0.8 V vs. SCE.

electrode 4 can be reduced, resulting in steady-state cathodic current at the collector electrodes. Consistent with expectation, the cathodic current when only electrodes 3 and 5 are used as collectors is the same as when electrodes 1–3 and 5–8 are used as collectors. Additionally, when electrodes 5–8 are used as collectors the cathodic current is only about one-half of that when electrodes 1–3 *and* 5–8 are used as collectors. Notice too that the anodic current at the generator electrode 4 depends on whether the collector electrodes are activated. When the collector electrodes are not activated the cyclic voltammogram at the generator electrode has a well-developed peak with a relatively small diffusional current on the positive potential side. When the collector electrodes are activated the cyclic voltammogram becomes closer to a steady-state current–voltage curve, at the scan rate illustrated. As will be developed below, the behavior of two microelectrodes connected with the same polymer, $PVFc^{+/0}$ or $(BPQ^{2+/+})_n$, is very different compared to the behavior of a pair of microelectrodes connected as illustrated in Scheme I. The crucial fact is that when the same redox polymer connects two microelectrodes the generator electrode and collector electrode can be interchanged, whereas when two different polymers connect two microelectrodes the generator and collector cannot be interchanged because large net current flow only occurs in one direction.

The steady-state current passing from one microelectrode to another when the two are connected by the same polymer depends on the charge transport properties of the polymer. As seen in Figure 4, the $PVFc^{+/0}$ system gives a steady-state current of the order of 1 nA when one microelectrode is held at +0.4 V vs. SCE where the ratio of $PVFc^{+}$ to $PVFc^{0}$ is about one to one and the

Scheme IV. Approximate Geometry Used To Determine D_{CT} Values for a Redox Polymer Connecting Two Adjacent Microelectrodes[a]

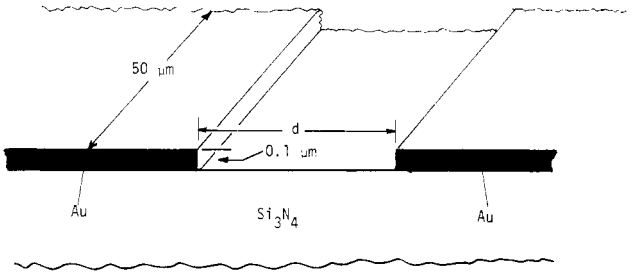

[a] The electrode area, A, is taken to be 0.1 μm × 50 μm = 5 × 10^{-8} cm^2.

adjacent electrodes are held at a potential of 0.0 V vs. SCE where the $PVFc^{+/0}$ polymer is in the $PVFc^{0}$ state. For the array characterized by the data in Figure 4 electron microscopy showed the polymer to be a thin, continuous, uniform coating over the microelectrodes at a thickness of ~0.3 μm. Assuming that the current observed is completely limited by the charge transport properties of the polymer, eq 3 approximates the expected current for a polymer of thickness d, diffusion coefficient for charge transport D_{CT}, transferring n electrons, and concentration of redox centers C.[12] The electrode area A is not perfectly well-defined by the geometry with the microelectrode arrays used here, because

$$i = nFAD_{CT}C/d \quad (3)$$

of the open-face sandwich structure. However, if we assume that the bulk of the current is associated with a 0.1 μm thickness of the polymer and the sides of the electrodes (the 0.1 μm × 50 μm area) give the electrode areas A, as illustrated in Scheme IV, the observed steady-state current gives a value of D_{CT} from the $PVFc^{+/0}$ polymer of $\sim 10^{-9}$ cm²/s in CH_3CN/0.1 M [n-Bu_4N]-ClO_4 for d = 1.0 μm and $C = 2.3 \times 10^{-3}$ mol/cm³.[8d] This accords well with existing literature[8] from conventional measurements where eq 3 can be more rigoriously applied because a one-dimensional diffusion model is realistic. We do not offer the microelectrode array as a superior geometry for determining D_{CT} values. Rather, what we stress here is that the steady-state currents found are reasonable in view of *known* values of D_{CT}.

The $(BPQ^{2+/+})_n$ polymer from I can also be used to connect two or more microelectrodes of an array. Basically, the procedure is to immerse the microelectrode array into the aqueous electrolyte solution of ~0.5 mM I and then cycle the potential (linearly, 50 mV/s) of the electrode(s) to be modified between 0.0 and −0.75 V vs. SCE. The negative excursion effects reductive deposition of the monomer, promoting polymerization to form the polysiloxane $(BPQ^{2+/+})_n$ polymer. Such deposited material is irreversibly bound to the array surface as evidenced by withdrawing the array from the derivatizing solution, rinsing with electrolyte solution containing no I, and examining the modified electrode(s) by cyclic voltammetry. Adjacent microelectrodes can thus become connected by the deposited[7] $(BPQ^{2+/+})_n$ polymer. This can be established by showing that steady-state current can pass between two microelectrodes coated with the $(BPQ^{2+/+})_n$ polymer, as has been demonstrated for $PVFc^{+/0}$-connected electrodes (Figure 4). The typical experiment would involve holding one microelectrode at 0.0 V vs. SCE, scanning the potential of the other (connected) microelectrode from 0.0 V vs. SCE in a negative direction to reduce the $(BPQ^{2+})_n$ polymer, and measuring the current passed through both interfaces.

The steady-state current passed between two $(BPQ^{2+/+})_n$-connected microelectrodes allows a determination of D_{CT} for the $(BPQ^{2+/+})_n$ polymer as described above for the $PVFc^{+/0}$ system. Again, the approximate value of D_{CT}, $\sim 10^{-9}$ cm²/s for $(BPQ^{2+/+})_n$, is in accord with the value recently reported.[9] Additionally, it is noteworthy that the value of D_{CT} for the $(BPQ^{+/0})_n$ redox level is determined to be higher than that for the $(BPQ^{2+/+})_n$ level, as was found earlier.[9] There is an increase in steady-state current of approximately a factor of at least 4 when holding one microelectrode at 0.0 V vs. SCE where the $(BPQ^{2+/+/0})_n$ system is in the $(BPQ^{2+})_n$ state and the other electrode is moved from −0.7 V vs. SCE where the $(BPQ^{+})_n$ level is maintained to a value of −1.1 V vs. SCE where the $(BPQ^{0})_n$ level is achieved. This experimental method does place the $2^{+/+}$ and $2^{+/0}$ states of the polymer in series, but this parallels the conventional experimentation published earlier.[9] More detailed studies of the microelectrodes connected with a single polymer will be reported elsewhere. The steady-state currents from the derivatized microelectrode arrays connected with the $(BPQ^{2+/+/0})_n$ polymer are in good agreement with known charge transport properties of the various redox levels of the polymer.

The values of D_{CT} for the $PVFc^{+/0}$ and $(BPQ^{2+/+})_n$ are found to be similar. Not only do the steady-state currents depend on the values of D_{CT} but also the switching time of a diode based on the arrangement in Scheme I depends on D_{CT}. The time for charge to traverse the distance d, t_d, is governed by eq 4. For D_{CT} values of 10^{-9} cm²/s and a distance of 1×10^{-4} cm the value of

$$d^2 = 2D_{CT}t_d \quad (4)$$

t_d is therefore 5 s. The switching time of a microelectrochemical diode device is therefore expected to be very slow compared to the speeds associated with solid-state devices having similar contact spacing.

Fabrication of a Two-Terminal Microelectrochemical Diode. To fabricate a diode the first step is to deposit Pt onto two adjacent microelectrodes in the desired amount. The second step is to electrochemically assist the deposition of $(BPQ^{2+/+})_n$ as previously described for macroscopic electrodes.[7] Figure 5 illustrates the

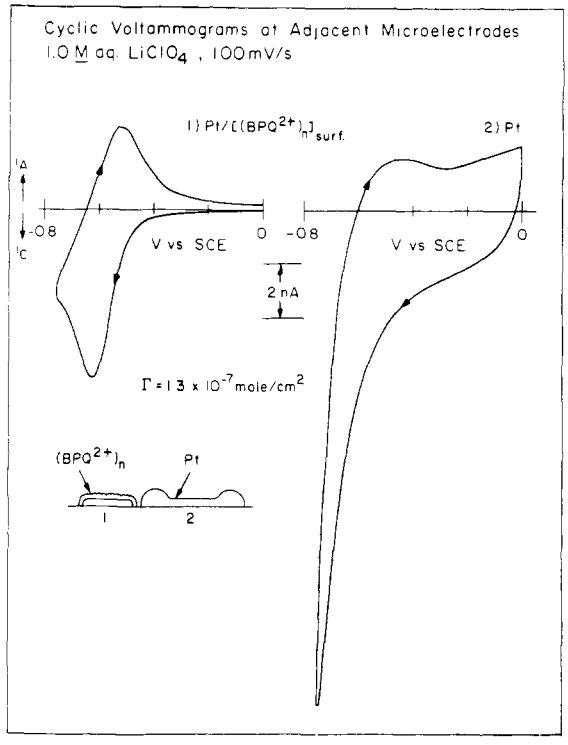

Figure 5. Cyclic voltammetry characterization of microelectrodes 1 and 2 after derivatization of electrode 1 with the $(BPQ^{2+/+})_n$ polymer. Electrode 2 shows no signal characteristic of the $(BPQ^{2+})_n \rightleftharpoons (BPQ^{+})_n$ like that found at electrode 1 (wave at −0.55 V vs. SCE). The large cathodic current at electrode 2 is H_2 evolution.

cyclic voltammetry response of a $(BPQ^{2+/+})_n$-modified microelectrode, electrode 1, adjacent to a microelectrode purposely not derivatized, electrode 2. The cyclic voltammetry for the $(BPQ^{2+/+})_n$-coated microelectrode is like that at a macroscopic electrode with a well-defined wave at ~−0.55 V vs. SCE corresponding to the $(BPQ^{2+})_n \rightleftharpoons (BPQ^{+})_n$ interconversion.[7] This establishes that the deposition of $(BPQ^{2+/+})_n$ can be controlled in the manner desired for fabrication of a device as represented in Scheme I. In order to keep electrode 2 free of $(BPQ^{2+/+})_n$, electrode 2 was held at 0.0 V vs. SCE where any BPQ^+ generated at electrode 1 would be oxidized. Thus, active potential control of electrode 2 prevents deposition of $(BPQ^{2+/+})_n$ while electrode 1 becomes modified. The deposited $(BPQ^{2+/+})_n$ on electrode 1 uniformly coats the microelectrode and "blocks" the access of $Ru(NH_3)_6^{3+}$ as illustrated in Figure 6. Figure 6 shows a comparison of the linear sweep current–potential curves at electrodes 1 and 2 before and after derivatization of electrode 1 with $(BPQ^{2+/+})_n$. Consistent with the lack of deposition of $(BPQ^{2+/+})_n$ onto electrode 2, electrode 2 shows the same response to $Ru(NH_3)_6^{3+}$ before and after derivatization of electrode 1. The response of electrode 1 to $Ru(NH_3)_6^{3+}$ after derivatization with $(BPQ^{2+/+})_n$ is in accord with the conclusion that the polymer completely covers electrode 1. The more negative onset for cathodic current corresponding to $Ru(NH_3)_6^{3+} \rightarrow Ru(NH_3)_6^{2+}$ reduction indicates that the reduced form of the polymer, $(BPQ^{+})_n$, is responsible for the reduction, as has been found at macroscopic electrodes derivatized with $(BPQ^{2+/+})$.[8] The $E^{\circ\prime}$ for $(BPQ^{2+/+})_n$ is ~−0.55 V vs. SCE compared to an $E^{\circ\prime}$ for $Ru(NH_3)_6^{3+/2+}$ of ~−0.16 V vs. SCE. The lower steady-state current for the reduction of $Ru(NH_3)_6^{3+}$ at the $(BPQ^{2+/+})_n$-coated electrode is in accord with the fact that the small value of D_{CT} for the polymer limits the steady-state current that can be passed through the interface.[9]

It is worth noting that the ability to purposefully alter the response of the $Ru(NH_3)_6^{3+/2+}$ at the $(BPQ^{2+/+})_n$-coated microelectrode allows a diode to be demonstrated.[13] The point is that two, "naked" microelectrodes are reversible to the $Ru(NH_3)_6^{3+/2+}$ couple. The $(BPQ^{2+/+})_n$-coated microelectrode only allows the reduction of $Ru(NH_3)_6^{3+}$ at a sufficiently negative

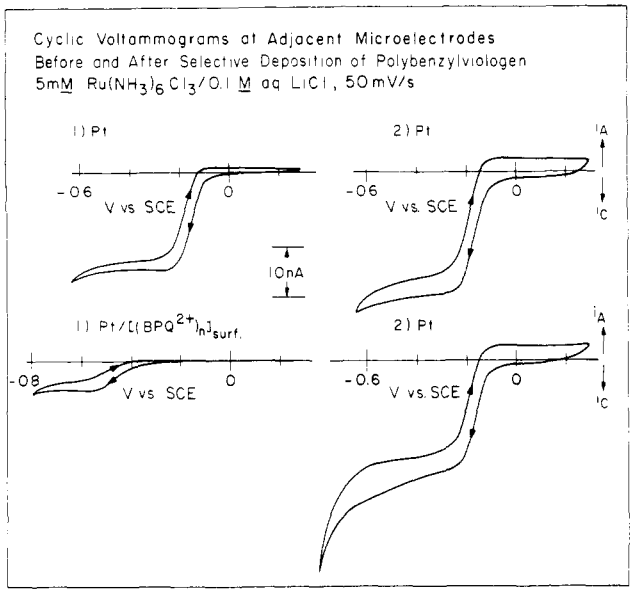

Figure 6. Comparison of the electrochemical response of electrodes 1 and 2 to $Ru(NH_3)_6^{3+}$ in aqueous electrolyte before (top) and after (bottom) derivatization of electrode 1 with $(BPQ^{2+/+})_n$ (cf. Figure 5). The response at electrode 2 is unaffected, since the $(BPQ^{2+/+})_n$ is only on electrode 1. The response at electrode 1 is changed in a manner consistent with reduction current occurring only via eq 5, i.e., reduction of $Ru(NH_3)_6^{3+}$ via (BPQ^+) units at the outermost portion of the polymer.

Scheme V. An Electrochemical Diode with One of the Redox Components, $Ru(NH_3)_6^{3+/2+}$, Dissolved in Solution and One Confined to One of the Microelectrodes, $(BPQ^{2+/+})_n$

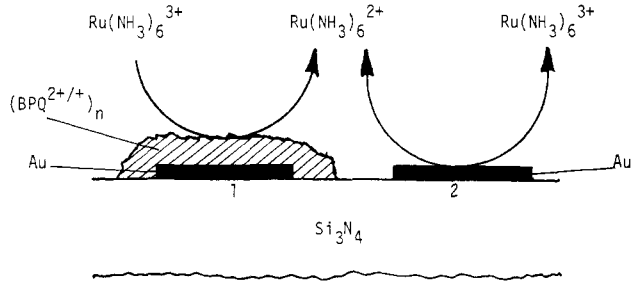

potential; the oxidation of $Ru(NH_3)_6^{2+}$ at a $(BPQ^{2+/+})_n$-coated microelectrode does not occur because BPQ^{2+} is too weak an oxidant and the positive charge of the complex prevents its penetration through the positively charged polymer to the surface of the Au. Thus, a device as represented in Scheme V constitutes a two-terminal diode with steady-state current flow effecting the reduction of $Ru(NH_3)_6^{3+}$ at the $(BPQ^{2+/+})_n$-coated microelectrode and oxidation of $Ru(NH_3)_6^{2+}$ at the naked microelectrode. For the diode represented by Scheme V, unidirectional electron transfer is found because the process represented by eq 5 is downhill by ~0.4 V; the reverse process is expected to be slow. However,

$$(BPQ^+)_n + nRu(NH_3)_6^{3+} \rightarrow (BPQ^{2+})_n + nRu(NH_3)_6^{2+} \quad (5)$$

since the $Ru(NH_3)_6^{3+/2+}$ is in solution the $(BPQ^{2+/+})_n$ polymer serves the additional function of preventing the solution redox system from contacting the metallic (reversible) electrode surface. The advantages of having both redox components immobilized as in the device represented by Scheme I are that there is no leakage from penetration of the solution reagent and that no solution redox reagent is required in order to achieve diode behavior. An advantage of the diode system shown in Scheme V is that the diffusion coefficient for the solution species is much greater ($\sim 10^{-6}$ cm^2/s for $Ru(NH_3)_6^{3+/2+}$ diffusion) than that for the bound polymer. The $(BPQ^{2+/+})_n$ properties remain limiting, but a polymer thickness of <1 μm can be useful, giving rise to faster switching times for the diode system shown in Scheme V.

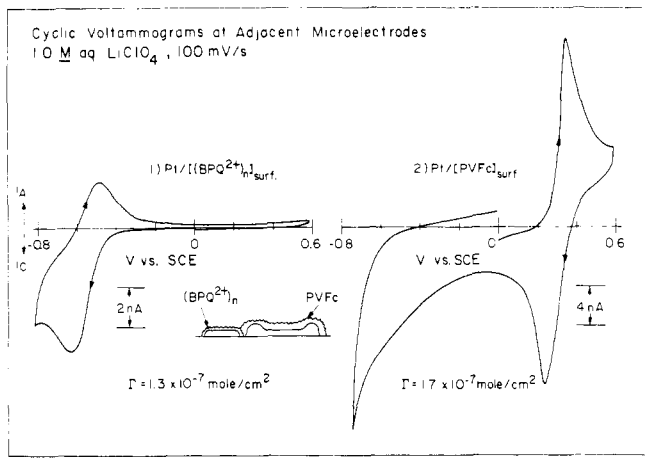

Figure 7. Cyclic voltammetry of electrodes 1 and 2 of the chip characterized by the data in Figures 5 and 6 after derivatization of electrode 2 with the $PVFc^{+/0}$ redox polymer. Note that electrode 1 shows the wave at −0.55 V vs. SCE characteristic of the $(BPQ^{2+})_n \rightleftarrows (BPQ^+)_n$ interconversion but no $PVFc^{+/0}$ wave (~+0.4 V vs. SCE) is observed. Electrode 2 shows a response characteristic of $PVFc^{+/0}$ redox polymer at ~+0.4 V vs. SCE. Data in Figure 8 establish that there is contact of the $(BPQ^{2+/+})_n$ polymer on electrode 1 with the $PVFc^{+/0}$ polymer on electrode 2.

After characterizing the $(BPQ^{2+/+})_n$-modified microelectrode as illustrated in Figures 5 and 6, the diode device is finished by functionalizing electrode 2 with a sufficient amount of $PVFc^{+/0}$ to make a connection to the $(BPQ^{2+/+})_n$ on electrode 1. Figure 7 shows the cyclic voltammetry characterization of electrodes 1 and 2 after such functionalization. Importantly, electrode 1 retains its $(BPQ^{2+/+})_n$ response but shows no response to $PVFc^{+/0}$ which would be found at ~+0.4 V vs. SCE; at the same time electrode 2 shows a response characteristic of $PVFc^{+/0}$ and still no response to the $(BPQ^{2+/+})_n$ on electrode 1. The result is that electrode 1 sees only $(BPQ^{2+/+})_n$ and electrode 2 sees only $PVFc^{+/0}$.

The data in Figure 7, however, do not establish that there is a connection of electrodes 1 and 2 by a $(BPQ^{2+/+})_n/PVFc^{+/0}$ contact. Figure 8 shows the crucial data in this regard. In the left-hand portion of the figure the currents at electrode 1 and 2 are shown for a potential excursion of electrode 1 from 0.0 to −0.8 V vs. SCE while the potential of electrode 2 is held at +0.4 V vs. SCE. The potential of electrode 2 is such that the ratio of $PVFc^0$ to $PVFc^+$ is about one. Thus, when the $(BPQ^{2+})_n$ on electrode 1 is reduced to $(BPQ^+)_n$ a current path between electrode 1 and 2 is possible according to eq 1. The right-hand side of the figure illustrates the data when the experiment is carried out such that electrode 1 is fixed at −0.6 vs. SCE where the $(BPQ^+)_n$ state is prevalent and electrode 2 is swept from 0.0 to +0.6 V vs. SCE. The currents again are consistent with a current path between electrodes 1 and 2 when the viologen on electrode 1 is reduced and the ferrocene on electrode 2 is oxidized. Steady-state current does not flow under other circumstances. In particular, if electrode 2 is moved negative of electrode 1 no current passes because $PVFc^0$ is thermodynamically incapable of reducing $(BPQ^{2+})_n$. The current–voltage curve for the scan of electrode 2 from 0.0 to +0.6 V vs. SCE is peak-shaped and does not plateau at the sweep rate shown. At slower sweep rates there is a plateau-shaped curve. The peak-shaped curve at 10 mV/s indicates the presence of excess polymer on the microelectrodes.

The final result of importance is the demonstration that a two-terminal device can actually show more steady-state current upon application of a potential in one direction than in the other. Figure 9 shows the data for steady-state current as a function of applied potential between electrodes 1 and 2. In this case there is no reference electrode and none is needed. Current will only pass when there is thermodynamically possible (and kinetically viable) chemistry that can occur. This situation is one where steady-state current can pass when the negative lead is connected to electrode 1 to effect $(BPQ^{2+})_n$ reduction and the positive lead is connected to electrode 2 to effect $PVFc^0$ oxidation. Regeneration

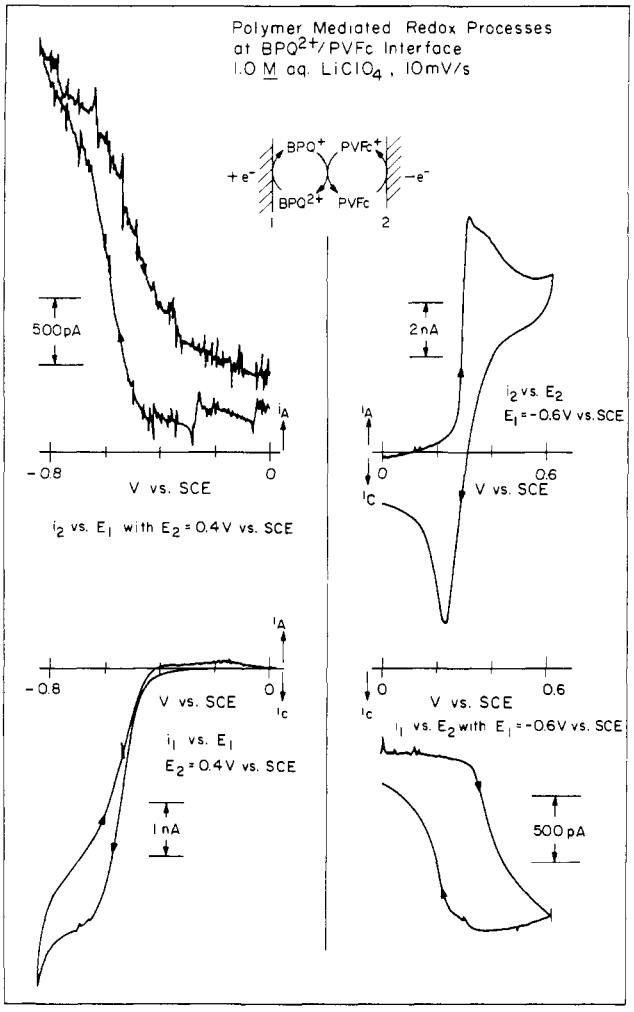

Figure 8. Demonstration that charge can be passed between microelectrodes 1 and 2 characterized by the data in Figure 7. The left portion of the figure shows the current–voltage behavior of electrode 1 while holding electrode 2 at +0.4 V vs. SCE (bottom) and the current at electrode 2 vs. the potential of electrode 1 (top). The right portion of the figure shows the current–voltage behavior of electrode 2 while holding electrode 1 at −0.6 V vs. SCE (top) and the current at electrode 1 vs. the potential of electrode 2 (bottom).

of $PVFc^0$ and $(BPQ^{2+})n$ occurs because the two polymers contact each other and react. The steady-state current through the two microelectrodes is consistent with the steady-state currents when only one polymer connects the two microelectrodes. This result means that the charge transfer rate at the $(BPQ^+)/PVFc^+$ interface is not rate limiting. A small current is observed upon application of a potential in the opposite direction and is presumably due to impurities in the H_2O electrolyte or to the onset of H_2O decomposition. Consistent with the low values of D_{CT} for $(BPQ^{2+/+})_n$ and $PVFc^{+/0}$ the switching time of the diode is of the order of seconds. An interesting result is the fact that the "turn on" voltage is close to that expected based on the difference in $E^{\circ\prime}$s for $(BPQ^{2+/+})_n$ and $PVFc^{+/0}$, ~0.9 V. Additionally, there is an inflection in the current–voltage curve at a voltage where the $(BPQ^0)_n$ redox level should be important. The increased current is presumably due to the fact that the $(BPQ^{+/0})_n$ level has a larger value of D_{CT} than does the $(BPQ^{2+/+})_n$ level.

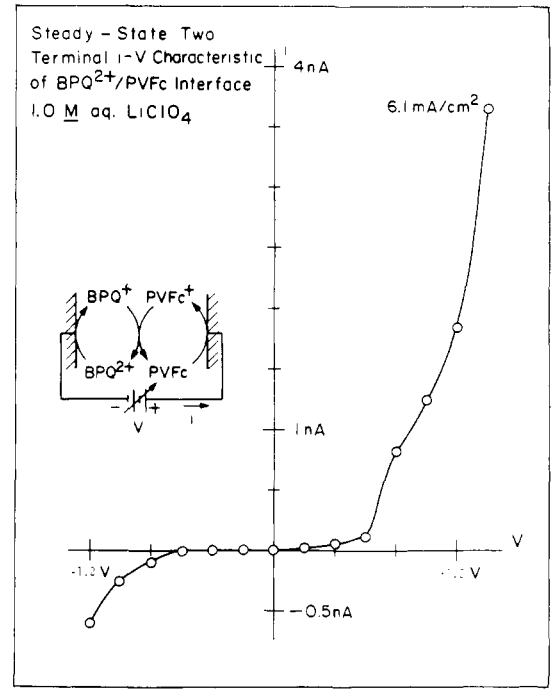

Figure 9. Two-terminal, steady-state current–voltage (diode) curve for the two-electrode chip characterized by the data in Figures 7 and 8. The right-hand portion of the current–voltage curve corresponds to the situation where the negative lead is attached to electrode 1, $(BPQ^{2+/+/0})_n$-coated, and the positive lead is attached to electrode 2, $PVFc^{+/0}$-coated.

Conclusions

The results presented above establish that it is possible to prepare an open-face sandwich analogue of bilayer electrochemical diodes[1] by connecting two closely spaced microelectrodes with an assembly of two different redox polymers such that the only mechanism for charge to pass from one microelectrode to another is via a polymer/polymer cross-redox reaction that is thermodynamically downhill. $PVFc^{+/0}$ or $(BPQ^{2+/+})_n$ can be deposited electrochemically, as on macroscopic electrodes,[8a,9] in a controlled fashion onto microelectrodes establishing electrochemical deposition of redox polymers to be a fabrication procedure for prototype devices. Another crucial feature of the fabrication methodology is the ability to control the deposition of Pt to close the gap between microelectrodes to values substantially less than 1 μm.

The data in Figures 8 and 9 establish that diode current–voltage curves can be obtained. However, the frequency of operation is slow by solid-state standards because of the known[8,9] small values of D_{CT} for redox polymers. The utility of this work rests not in the fabrication of useful diodes but in the demonstration that relatively simple molecule-based components can be assembled and contacted to achieve a function. More "useful" microelectrochemical diodes are under study in these laboratories with particular emphasis on diodes based on redox components where the steady-state current can be modified by the chemicals in the medium into which the diode is immersed.

Acknowledgment. We thank the Office of Naval Research and the Defense Advanced Research Projects Agency for partial support of this research. We also thank Robert Radway and Russell McDonnell for their assistance in photolithography, metal deposition, and metal lift-off procedures.